

Optimization of Tensile Response of Wood Ash Particles Reinforced Polypropylene (WARPP) for Auto Part Design

Chukwutoo C. Ihueze¹, Patrick S. Aguh²

^{1,2}Department of Industrial and Production Engineering, NnamdiAzikiwe University Awka, Anambra State, Nigeria

Abstract

The study focused on the use of response surface methodology to predict the optimal tensile response of wood ash particles /polypropylene combination for auto part (car bumper) design. Taguchi plan of experiment based on $L_9(3)^4$ was used to design the experiment. The data obtained from the experiment were analyzed using S/N ratio and mean of means as the statistical measure of performance. The response surface and contour plots show the optimized responses of individual interactions in the range of $> 13.50\text{MPa}$ - $> 19.50\text{MPa}$. The contour and surface plots depict the behaviour of the tensile strength as two input variables vary and two held constant at their highest settings). The tensile strength of WARPP is in the range of 17.08MPa - 21.19MPa . The highest tensile strength value was obtained by simultaneous optimization of input variables depicted in optimization plot of figure 15 as 21.19MPa . Further investigations are recommendable for testing WARPP under high temperature for the design/formulation of auto part (car bumper) to ascertain its performance at elevated temperature.

Keywords: Optimization, Experimental design, Taguchi method, Performance characteristics, Box-Behnken design, Interaction plots, TRD-RSM.

I. INTRODUCTION

Bumpers made of composite materials are now replacing the steel bumpers that stay back in low strength to weight ratio. Production of composite bumpers has been attempted using plastic – thermoset. An auto part structure like bumper, capable of increased energy absorption over metal, is being increasingly exploited within automotive structures. The discovery and application of composite materials dated back some years ago. The earliest scientific discovery of composite materials was discussed by Amstead et al (1979) and Vaidya(1988). Further discussions on the development and engineering use of composite were made by Strong, Jonson, Avallone and Baumeister (1997). The engineering application of composites dated back to the use of straw in clay by the Egyptians and Mesopotamian settlers to create strong and durable buildings. The application of straw was

extended to reinforcing ancient composite products such as pottery and boats.

Okunade (2008) in his research article titled ‘the effect of wood ash and saw – dust admixtures on the engineering properties of a burnt laterite – clay brick’ stated that wood ash admixture in line with its pozzolanic nature was able to contribute in making denser products with higher compressive strengths. Naik et al (2001) studied wood ash as a new source of pozzolanic material. He experimented on the physical, chemical and micro structural properties of wood ash in order to determine the potential application for it.

Goodman Mark Mendel conducted research on the effects of wood ash additive on the structural properties of lime plaster. He evaluated two samples of ashes obtained from animal dung and hardwoods. The variation inherent in the dung ash was such that it cannot be replicated. Wood ash engineering application has been studied relatively by few researchers.

In this study wood ash particles / polypropylene was used for car bumper design. Taguchi experimental design technique was applied in the design and data were analyzed using S/N ratio. The Taguchi robust design was used to plan a minimum number of experiments needed to optimize the performance characteristics of WARPP. Response surface plots and contour plots were used for this optimization.

A bumper is a shield or protector made of steel, aluminum, rubber or plastics that are mounted on the front and rear parts of a passenger car (Prabhakaran et al 2012). Bumper systems are attached to vehicles to absorb the impact shock during low speed collision and also to reduce damage to the internal part of vehicle. Bumpers have been improved upon by the design and use of composite material to achieve high performance.

II. METHODOLOGY

A. Experimental Design

The method applied in this study followed experimental design technique of Taguchi robust design in f planning and conducting experiments and analyzing

the data. In planning, Taguchi $L_9(3)^4$ orthogonal array for four design factor presented in table I were used to set up the experiment. The design parameter matrix specified the test settings of the design parameters. The four design factors: particle size, volume fraction, injection force and operating temperature, each tested at three levels for nine test runs. The noise factors likely to affect the performance of the product include temperature, humidity and operator.

Table I : $L_9(3)^4$ Orthogonal Array of Design Parameters

Expt. No.	Factor A: Particle Size, (mm)	Factor B: Volume fraction, (%)	Factor C: Injection force, (ton.)	Factor D: Operating temp. ($^{\circ}\text{C}$)
1	0.25	5	120	185
2	0.25	35	160	200
3	0.25	60	200	215
4	0.80	5	160	215

5	0.80	35	200	185
6	0.80	60	120	200
7	1.40	5	200	200
8	1.40	35	120	215
9	1.40	60	160	185

B. Sample Preparation and Conduct of Experiment

The replicated samples of wood ash particles reinforced polypropylene (WARPP) produced in an injection moulding machine were used to conduct experiment. The injection moulding process variables considered in the production of the samples were categorized as plastic variables and machine variables. The samples produced were tested for tensile failure (ultimate stress), and the results are presented in table II.

TABLE II : Experimental Results of the Trial Tests of Warpp

Exp.	Particle size, (mm)	Volume fraction, %	Injection force, ton	Melt Temp, $^{\circ}\text{C}$	Performance characteristics of trial tests.				
					Trial 1	Trial 2	Trial 3	Trial 4	Trial 5
1	0.25	5	120	185	13.89	13.89	11.81	13.89	12.50
2	0.25	35	160	200	12.50	15.27	13.89	18.06	16.67
3	0.25	60	200	215	15.28	13.89	11.81	12.50	12.50
4	0.80	05	160	215	19.44	17.36	18.75	18.06	18.75
5	0.80	35	200	185	6.94	18.75	19.44	15.97	15.27
6	0.80	60	120	200	13.89	15.28	18.06	18.06	18.06
7	1.40	5	200	200	9.72	12.50	9.72	9.72	13.89
8	1.40	35	120	215	18.06	11.67	13.19	19.44	15.28
9	1.40	60	160	185	20.83	20.83	20.83	20.83	20.83

C. Determination of Tensile Properties

Each of the sample replications' described in table II as trials 1, 2, 3, 4 and 5, were subjected to tension loading individually in the testing kit of a universal Monsanto extensometer. The appropriate beam loaded of 2500N (250Kgf) was applied each time by the operator through the operating handle. Readings of displacements (extensions) versus loads were obtained from the autographic recording paper. From the readings the ultimate stress or tensile strength of the samples were identified as the failure points of the samples. The performance characteristic is evaluated for each of the five tests (trials), and performance statistics like the mean and the signal - to - noise (S/N) ratio were determined and presented as shown in table III.

The mean response (tensile strength) of table III is computed from the data of table II. The mean

standard deviation (MSD) and S/N ratio as shown in table III were computed using the relations:

$$MSD = \left(\frac{1}{n} \sum_{i=1}^n \frac{1}{y_i^2} \right) \quad (1)$$

and

$$S/N_i = -10 \log \left(\frac{1}{n} \sum_{j=1}^n \frac{1}{y_{ij}^2} \right) \quad (2)$$

Where n = number of experimental trials, y_i = performance characteristics, MSD = mean square deviation.

Table III : Experimental Results of Performance Characteristics of Tensile Strength & S/N Ratio.

Expt. No.	Particle size, A (mm)	Volume fraction, C (%)	Injection force, C (Ton)	Oper. temp., D (°C)	Mean tensile (Mpa)	MSD	S/N ratio
1	0.25	5	120	185	13.196	0.0058	22.35
2	0.25	35	160	200	15.278	0.0045	23.46
3	0.25	60	200	215	13.196	0.0059	22.30
4	0.80	5	160	215	18.472	0.0029	25.31
5	0.80	35	200	185	15.274	0.0069	21.62
6	0.80	60	120	200	16.67	0.0037	24.28
7	1.40	5	200	200	11.11	0.0087	20.62
8	1.40	35	120	215	15.528	0.0046	23.36
9	1.40	60	160	185	20.83	0.0023	26.37

The mean response of the S/N ratio and mean of means of tensile test evaluated at different levels of factors are shown in table IV.

Table IV : Responsetable For S/N Ratio and Mean of Means of Tensile Tests Results.

Level	S/N				Mean of means			
	A (mm)	B (%)	C (N)	D (°C)	A (mm)	B (%)	C (N)	D (°C)
1	22.70	22.76	23.33	23.45	13.89	14.26	15.13	16.43
2	23.74	22.81	25.05	23.70	16.81	15.36	18.19	14.35
3	23.45	24.32	22.43	23.66	15.82	16.90	13.19	15.73
Delta	1.04	1.56	2.62	0.25	2.92	2.64	5	2.08
Rank	3	2	1	4	2	3	1	4

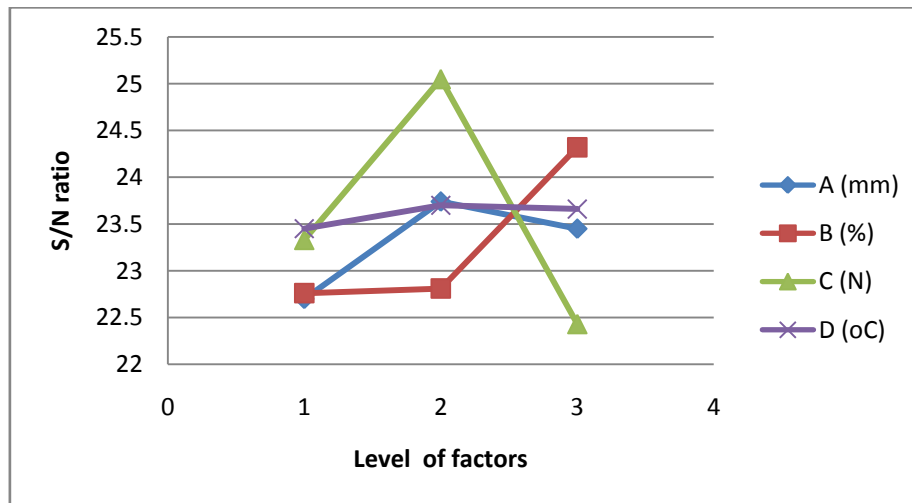


Fig. 1 Main Effect Plot of S/N Ratio of Tensile Response for Greater the Better.

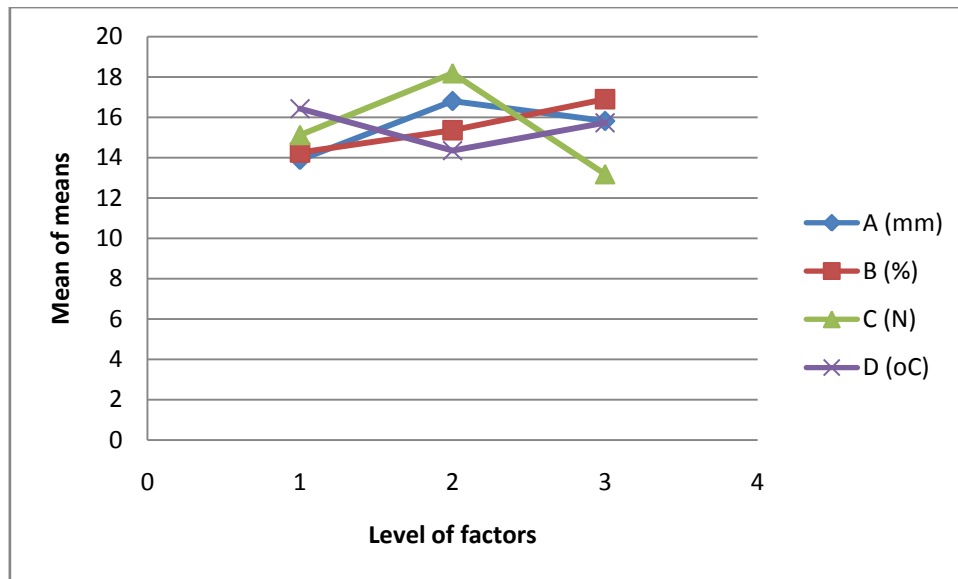


Fig. 2 Main effect Plot of Mean of Means of Tensile Response for Greater the Better

D. Evaluation of Expected Response

The relation for evaluation of expected response of Taguchi robust design is reported by

$$ER = AVR + (A_{opt} - AVR) + (B_{opt} - AVR) + (C_{opt} - AVR) + (D_{opt} - AVR) \quad (3)$$

$$AVR = \frac{A_{opt} + B_{opt} + C_{opt} + D_{opt}}{4} \quad (4)$$

Where

AVR = average response evaluated at optimum setting of factors,

D_{opt} = optimum value of response at optimum setting of factor D.

Applying the data values of table IV with (3) and (4), the expected values of tensile strength responses are obtained as summarized in table V.

Table V : Optimal Setting and Expected Values of Responses.

Response	A_{opt}	B_{opt}	C_{opt}	D_{opt}	AVR	ER	Levels
Tensile	16.81	16.90	18.19	16.43	17.0825	17.08	A2,B3,C2,D1

E. Optimization of Performance Characteristics

The use of response surface method was adopted because of the limitation of Taguchi method of not handling interaction effects of factors. The response surface method (RSM) used to handle noise effects can be solved involving two approaches in the manner presented in this study. In this study the data obtained from Taguchi robust design is linearized on the assumption that the experimental results follow a power law model of the form

$$Y = a_0 X_1^{a_1} X_2^{a_2} X_3^{a_3} \dots X_n^{a_n} \quad (5)$$

and that the response surface is optimized by a second order polynomial also expressed as

Radharamanan and Ansuji (2001) and can be expressed for four control factor experiment as:

A_{opt} = optimum value of response at optimum setting of factor A,

B_{opt} = optimum value of response at optimum setting of factor B,

C_{opt} = optimum value of response at optimum setting of factor C and

$$\hat{Y} = \beta_0 + \sum_{i=1}^K \beta_i X_i + \sum_{i=1}^k \beta_{ii} X_i^2 + \sum_{i=1}^{k-1} \sum_{j=2}^k \beta_{ij} + \epsilon \quad (6)$$

For four control factors and three levels design (5) reduces to

$$Y = a_0 X_1^{a_1} X_2^{a_2} X_3^{a_3} X_4^{a_4} \quad (7)$$

and (6) reduces to

$$\hat{Y} = \beta_0 + \beta_1 X_1 + \beta_2 X_2 + \beta_3 X_3 + \beta_4 X_4 + \beta_{11} X_1^2 + \beta_{22} X_2^2 + \beta_{33} X_3^2 + \beta_{44} X_4^2 + \beta_{12} X_1 X_2 + \beta_{13} X_1 X_3 + \beta_{14} X_1 X_4 + \beta_{23} X_2 X_3 + \beta_{24} X_2 X_4 + \beta_{34} X_3 X_4 \quad (8)$$

By linearizing the experimental responses of the tensile results of table III the following power law

model is obtained for the tensile performance characteristics.

$$Y_{ten} = 325,644.2814 X_1^{-0.02499} X_2^{-0.00436} X_3^{-0.55694} X_4^{-1.34015}$$

The power law model of (9) was used to evaluate the design matrix of Box – Behnken design and presented in table VI.

Table VI: Design Matrix of Box – Behnken Design and Power Equation of Tensile Strength Ofwarpp.

Std. order	Run order	Particle size, A (mm)	Vol. fraction, B (%)	Inject. Force, C (ton)	Operat. Temp. D (°C)	Response, Y Ten. (MPa)
9	1	0.250	32.5	160	185	18.0004
22	2	0.825	60.0	160	185	17.4246
15	3	0.825	5.0	200	200	14.0125
13	4	0.825	5.0	120	200	18.6240
10	5	1.40	32.5	160	185	17.2418
3	6	0.250	60.0	160	200	16.1714
18	7	1.40	32.5	120	200	18.2302
11	8	0.250	32.5	160	215	14.7168
4	9	1.40	60	160	200	15.4899
17	10	0.250	32.5	120	200	19.0322
26	11	0.825	32.5	160	200	15.7380
21	12	0.825	5.0	160	185	17.6142
25	13	0.825	32.5	160	200	15.7380
24	14	0.825	60.0	160	215	14.2461
1	15	0.250	5.0	160	200	16.3473
19	16	0.250	32.5	200	200	14.3197
20	17	1.40	32.5	200	200	13.7162
6	18	0.825	32.5	200	185	15.4295
14	19	0.825	60.0	120	200	18.4235
5	20	0.825	32.5	120	185	20.5072
7	21	0.825	32.5	120	215	16.7664
2	22	1.40	5.0	160	200	15.6585
8	23	0.825	32.5	200	215	12.6149
12	24	1.40	32.5	160	215	14.0967
27	25	0.825	32.5	160	200	15.7380
16	26	0.825	60.0	200	200	13.8617
23	27	0.825	5.0	160	215	14.4011

1) **Interaction plots – Response surface and Contour Modeling**

The interaction plots of design variables for tensile responses are depicted graphically in figures 3 – 14.

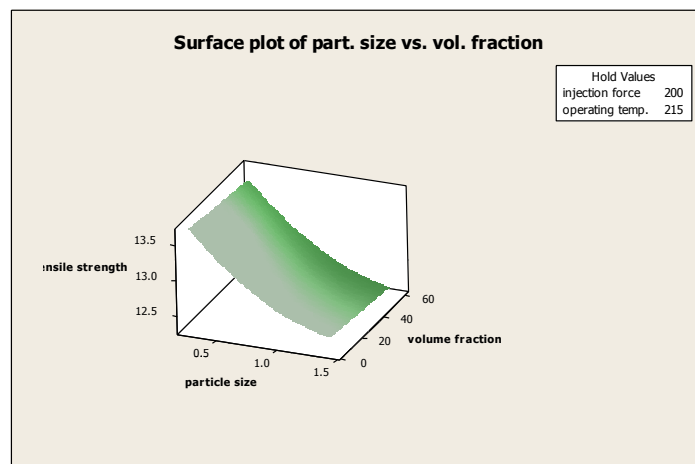


Fig. 3 Surface Plot of Tensile Strength Vs. Particle Size & Volume Fraction

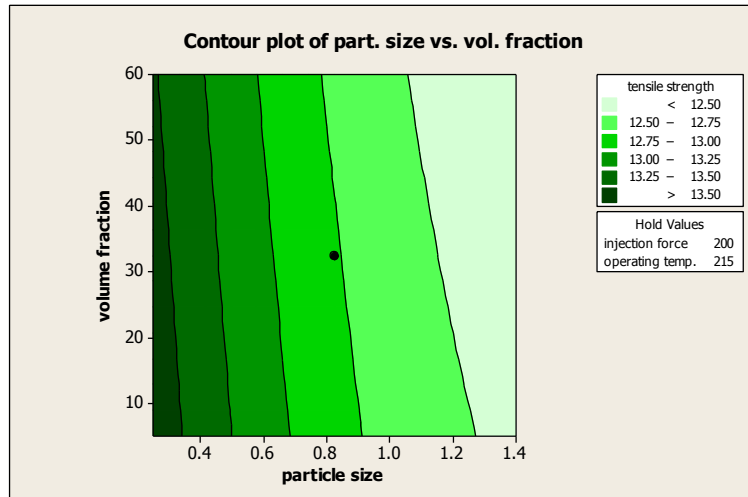


Fig. 4 Contour Plot of Particle Size Vs. Volume Fraction

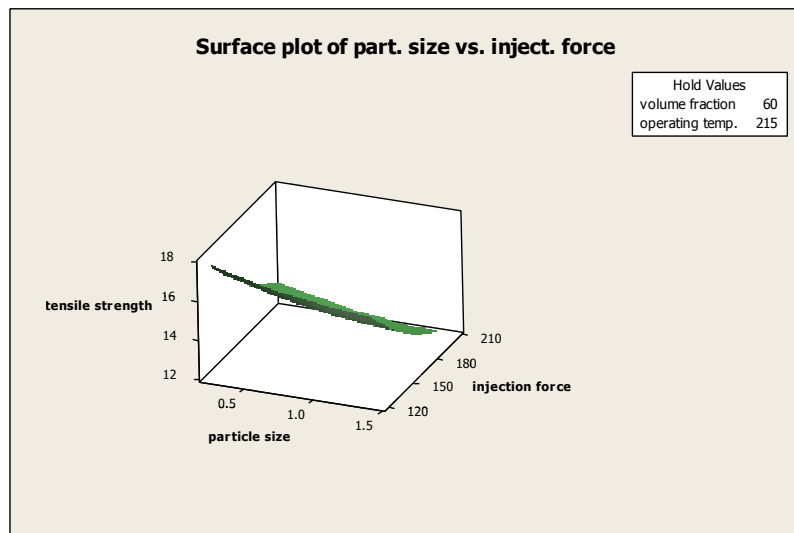


Fig. 5 Surface Plot of Tensile Strength Vs. Particle Size & Injection Force

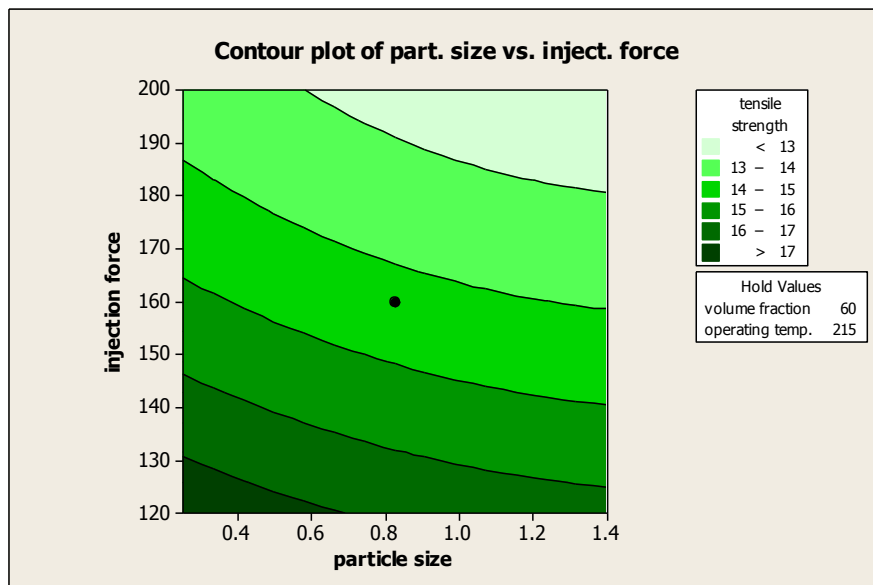


Fig. 6 Contour Plot of Particle Size Vs. Injection Force

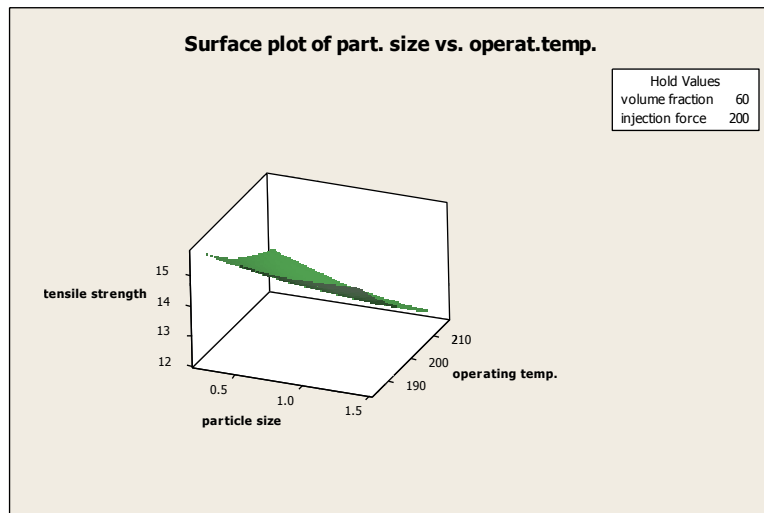


Fig. 7 Surface Plot of Tensile Strength Vs. Particle Size & Operating Temperature

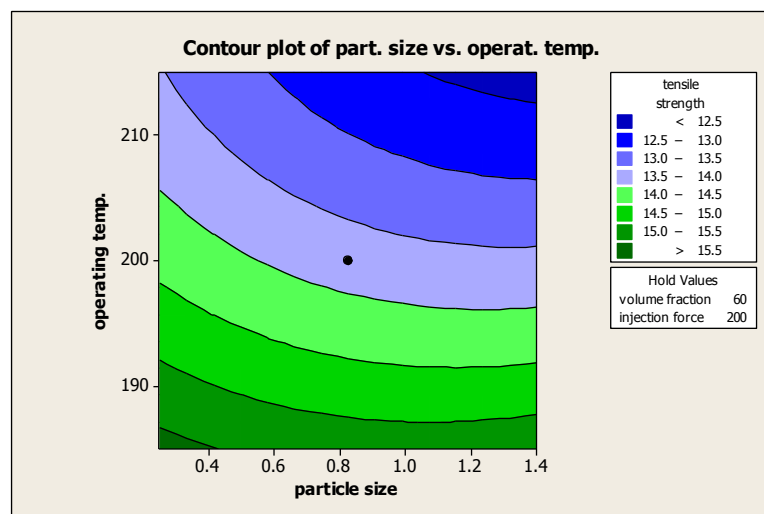


Fig. 8 Contour Plot of Particle Size Vs. Operating Temperature

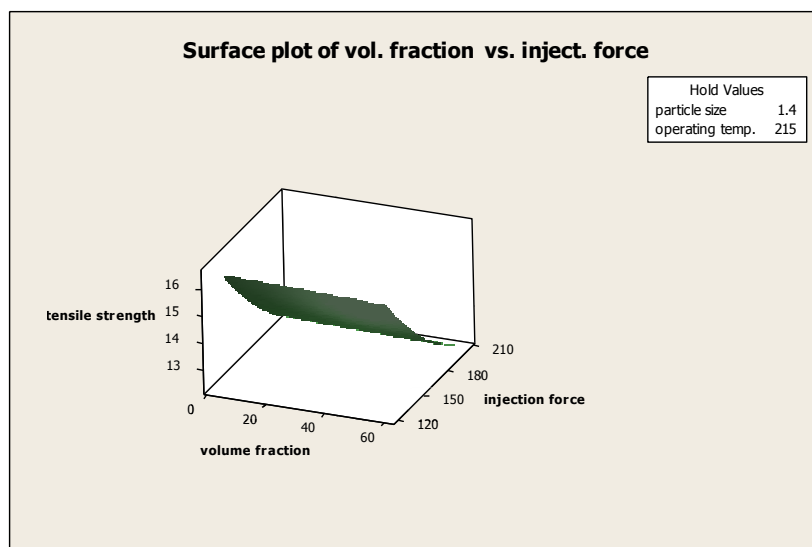


Fig. 9 Surface Plot of Tensile Strength Vs. Volume Fraction & Injection Force

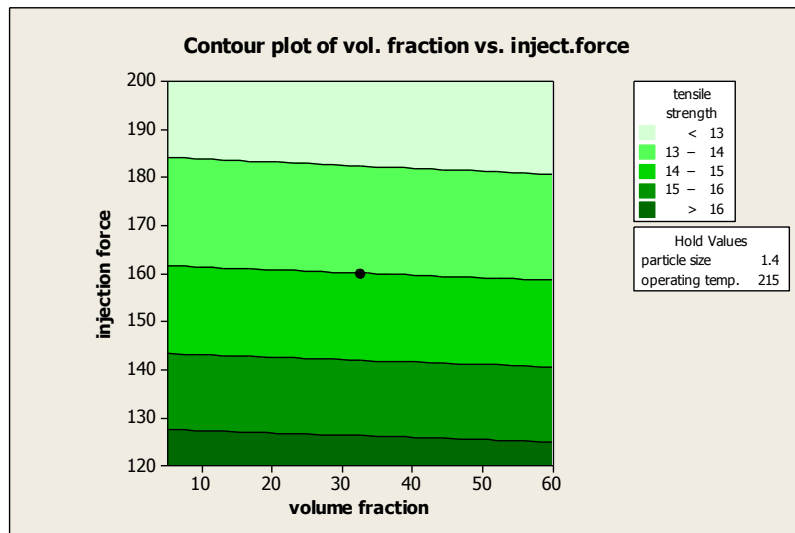


Fig. 10 Contour Plot of Volume Fraction Vs. Injection Force

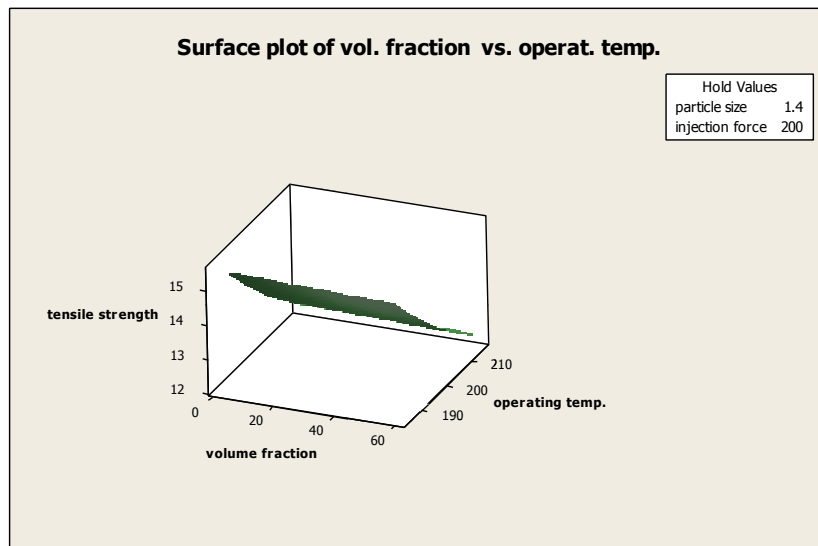


Fig. 11 Surface Plot of Tensile Strength Vs. Volume Fraction & Operating Temp

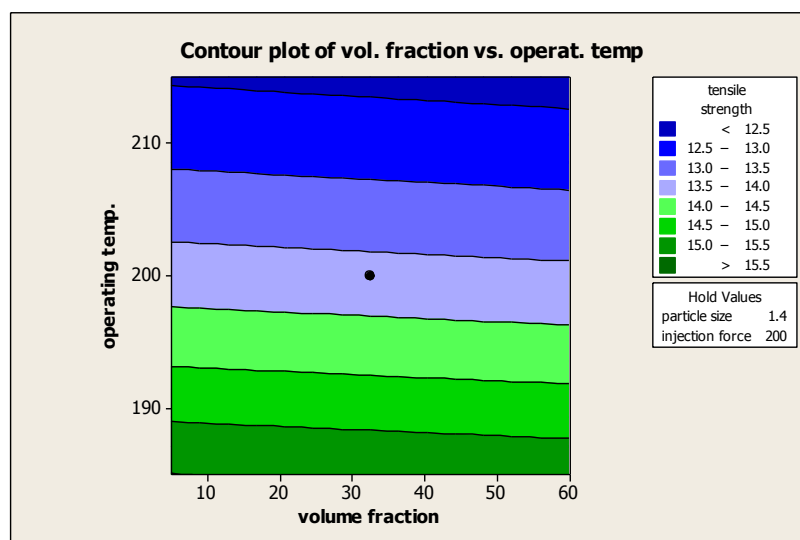


Fig. 12 Contour Plot of Volume Fraction Vs. Operating Temperature

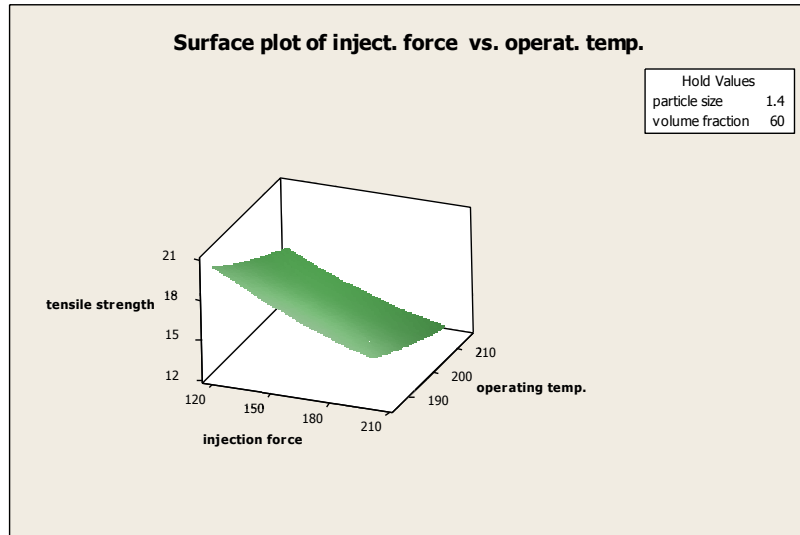


Fig. 13 Surface Plot of Tensile Strength Vs. Inject. Force & Operating Temperature

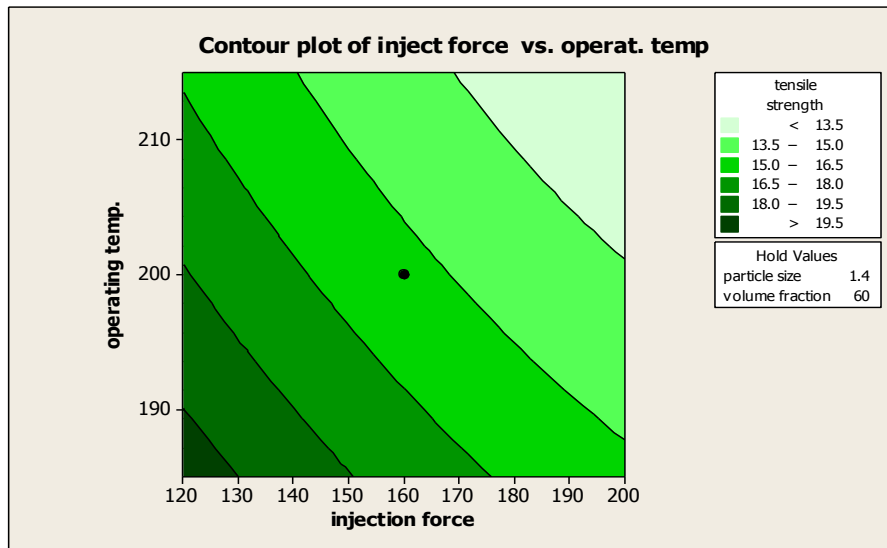


Fig. 14 Contour Plot of Injection Force Vs. Operating Temperature.

2) **Desirability Function and Optimization**

The optimum variables of tensile response of WARPP are shown in the following figure.

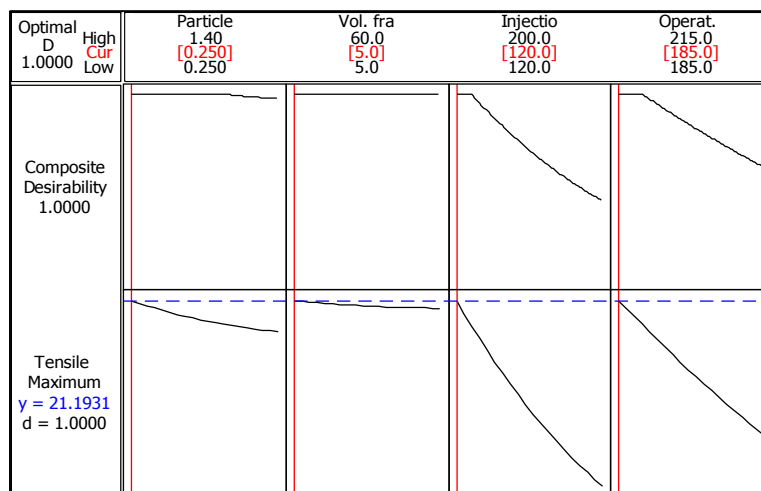


Fig. 15 Minitab 16 Depiction of Optimum Values of Factors for Optimum Tensile Response.

III. DISCUSSION OF RESULTS

The response surface model of the tensile response of RSM is in the form of equation (8) and expressed as in table 3 VII.

As can be seen from table VIII the F- values obtained is greater than the F- value (2.64 at 95% significance) obtained from a standard distribution table, confirming the adequacy of the model fits. Significance of each term in the models is determined with the p-value associated with the terms. A term is not significant if p-value is greater than 0.05 as depicted in tables VIII. Analysis of variance (ANOVA) subdivides the total variation of results into two Sources of variation, namely the regression model and residual (experimental) error. ANOVA shows whether the variation from model is significant when compared to the variation due to residual error. The F-test value is used for this analysis.

The predicted R² is a measure of how good the model predicts a response value. The adjusted R² and predicted R² should be within 0.20 of each other to be in reasonable agreement (Mourabet et al., 2013) as depicted in table IX for tensile response of WARPP, showing that model of table VII is perfect fits of experimental results.

The interaction effects of table X show the local solutions (optimized responses) of individual interactions. By simultaneous optimization the global solution of figure 15 is obtained.

The results of the two methods of this study are summarized in table XI with TRB-RSM giving higher results than the TRD.

Table VII : Estimated Regression Coefficient Of Model.

Term	Y _{ten} - Coefficient
Constant	93.1261
A	-2.43198
B	-0.01291
C	-0.22699
D	-0.42347
AA	0.41091
BB	5.62920E-05
CC	2.81536E-04
DD	6.25204E-04
AB	1.15415E-04
AC	2.15761E-03
AD	4.01449E-03
BC	1.12955E-05
BD	2.09697E-05
CD	3.85958E-04

Table VIII : Analysis of Variance (Anova) for Tensile Strength of Warpp.

Source	DF	Seq SS	Adj SS	Adj MS	F	p
Regression	14	97.8109	97.8109	6.9865	19184.73	0.000
Linear	4	96.4267	96.4267	24.1067	66196.28	0.000
A	1	1.4383	1.4383	1.4383	3949.60	0.000
B	1	0.0902	0.0902	0.0902	247.69	0.000
C	1	63.6130	63.6130	63.6130	174679.67	0.000
D	1	31.2851	31.2851	31.2851	85908.17	0.000
Square	4	1.1541	1.1541	0.2885	792.31	0.000
A*A	1	0.0006	0.0984	0.0984	270.31	0.000
B*B	1	0.0708	0.0097	0.0097	26.54	0.000
C*C	1	0.9772	1.0822	1.0822	2971.70	0.000
D*D	1	0.1055	0.1055	0.1055	289.80	0.000
Interaction	6	0.2301	0.2301	0.0383	105.30	0.000
A*B	1	0.0000	0.0000	0.0000	0.04	0.852
A*C	1	0.0099	0.0099	0.0099	27.05	0.000
A*D	1	0.0048	0.0048	0.0048	13.17	0.003

<i>B*C</i>	1	0.0006	0.0006	0.0006	1.70	0.217
<i>B*D</i>	1	0.0003	0.0003	0.0003	0.82	0.382
<i>C*D</i>	1	0.2145	0.2145	0.2145	589.03	0.000
<i>Residual error</i>	12	0.0044	0.0044	0.0044		
<i>Lack of fit</i>	10	0.0044	0.0044	0.0044		
<i>Pure error</i>	2	0.0000	0.0000	0.0000		
<i>Total</i>	26	97.8153				

Table IX : Regression Statistics for Tensile Strength

<i>Std. dev.</i>	0.0190832	<i>R – squared (pred.)</i>	99.97 %
<i>PRESS</i>	0.0251714	<i>R – squared (adj.)</i>	99.99 %
<i>R – squared</i>	100 %		

Table X : Interaction Effects of Variables for Tensile Response of Warpp.

Interaction variables	Response value (MPa)	Hold values of A, B, C and D
A*B	> 13.50	C (200), D (215)
A*C	> 17.00	B (60), D (215)
A*D	> 15.50	B (60), C (200)
B*C	> 16.00	A (1.4), D (215)
B*D	> 15.50	A (1.4), C (200)
C*D	> 19.50	A (1.4), B (60)

Table XI : Summarized Response of Method.

Methods			Optimum setting of factors (A, B, C,D)			
Response	TRD	TRD-RSM	Levels			
Y_{ten} (Mpa)	17.08	21.19	0.25mmm	5%	120 ton	185 °C

IV. CONCLUSION

The following conclusions are therefore drawn

- The tensile strength of WARPP is in the range 17.08Mpa – 21.19Mpa.
- The surface response and contour plots show the local solutions (optimized responses) of individual interactions of variables in the range of > 13.50Mpa – 19.50Mpa.
- The response model of WARPP for tensile is representable with nonlinear power law model and second order polynomial model.
- Further investigations are recommended for testing WARPP under high temperature applications to ascertain its performance at elevated temperatures.

REFERENCES

[1] Amstead B.H., Ostwald P.F. and Begeman M.L. (1979), Manufacturing Processes; John Wiley and Sons Inc. p 256.
 [2] Avallone E.A., Baumeister T. III (1997), Marks Standard Handbook for Mechanical Engineers, 10th Edition, McGraw Hill book company, Singapore, p 6-202.
 [3] Bertoline G. R., Wiebe E. N., Miller C. I., Mohler J. I. (1997). Technical Graphics Communication. McGraw Hill Company pp 948 – 949.
 [4] Goodman M. M. (1998). The effects of Wood Ash Additive on the Structural Properties of Lime plaster. [http://archive.org/stream/effectsofwoodashoogood/efects of woodash](http://archive.org/stream/effectsofwoodashoogood/efects%20of%20woodash).
 [5] Naik T. R., Kraus R., and Kumar R. (2001), Wood Ash: A New Source of Pozzolanic Material. Report No. CBU 2001

Center for By- product Utilization. University of Wisconsin.
 [6] Okunade E. A., (2008), The effect of Wood Ash and Sawdust Admixture on the Engineering Properties of a Burnt Laterite Clay. Journal of Applied Sciences, 8: 1042 – 1048.
 [7] Prahakaran K., Chinnarasu M., Senthil K., (2012) ‘for Design and Fabrication of Composite Bumper Light Passenger Vehicle’. International Journal of Modern Engineering Research Vol. 2 issue 4 pp 2552 -2556.
 [8] Radharamanan R. and Ansui A. P. (2001), ‘Quality improvement of a production process using Taguchi methods’, Proceedings of Institute of Industrial Engineers Annual Conference, Dallas, Texas, 20 – 22.
 [9] Vaidya A.A. (1988), Production of Synthetic Fibers Prentice-Hall of India Private Ltd, New Delhi.